Robotica (2009) volume 27, pp. 779–788. © 2008 Cambridge University Press
doi:10.1017/S0263574708005195 Printed in the United Kingdom

Design and realization of a snake-like robot system based on a spatial linkage mechanism

Na Li, Tieshi Zhao*, Yanzhi Zhao and Yongguang Lin

College of Mechanical Engineering, Yanshan University, Qinhuangdao 066004, P.R. China

(Received in Final Form: October 2, 2008. First published online: November 10, 2008)

SUMMARY

This paper presents a novel model of snake-like robots based on a spatial linkage mechanism. The reasonable structural parameters of the mechanism are obtained by performing a kinematic simulation. Then the kinematics of the spatial linkage mechanism is developed and the motor angles of the robot for performing lateral undulation are analyzed based on the Serpenoid curve. The torque of servomotors at each moment is also obtained. The experiments detailed in this paper confirm that the robot is of the ability to realize several motion modes, including lateral undulation, left and right turning motions, and uplifting of the head.

KEYWORDS: Snake-like robot; Spatial parallel mechanism; Kinematics; Locomotive gait; Motion control.

1. Introduction

In nature, biologic snakes are able to move nimbly in various complex environments because of their flexible and slender characteristics. On the basis of the imitation of these features, snake-like robots are suitable for hazardous search and rescue tasks, such as fire fighting, earthquake rescue, battlefield scouting, and so on. However, the research on snake-like robots presents a number of technical research challenges, specifically the design of mechanism for satisfying the requirements of flexibility. A biologic snake has more than 200 vertebras (modules), and each two vertebras are articulated by a ball-and-socket joint, and so it moves with high flexibility. But under current conditions of technique, it is difficult to develop and control a snake-like robot with so many vertebras and ball-and-socket joints. Therefore, the design and control of snake-like robots have been attracting much attention of many researchers.

Generally, a snake-like robot consists of a large number of homogeneous modules, which is considered to be of a particular class of hyper-redundant robots.[1,2] Because of their highly articulated structures, many snake-like robots are designed as modular and reconfigurable systems, which simplify the process of design, manufacturing, control, and maintenance, and also make snake-like robots suitable for more arduous tasks. There have been a variety of modular reconfigurable systems proposed and established,[3–8] which are applicable in the design and construction of snake-like robots for enhancing functionality and versatility. The architectures of snake-like robots are mostly based on "discrete backbone" that comprises a number of rigid linkages.[9] Earlier the modules were usually connected by revolute joints with parallel axes, and thus robots could only realize planar movements. Recently, most snake-like robots[10–12] are based on the adjacent orthogonal serial mechanism, where the axes of each two adjacent revolute joints are orthogonal. With this simple serial mechanism, the robots can implement either planar locomotion or spatial locomotion.[13,14] Some snake-like robots with universal joints[15] have the capability to realize more complicated three-dimensional motion, but they have the difficulty of fixing two servomotors corresponding to the two axes of the universal joints. There also have been some snake-like robots designed to imitate the high flexibility of snakes. One of the S-series snake-like robots built by Gavin Miller is composed of different shape modules[16] and aims at obtaining high maneuverability and flexibility. The first GMD snake-like robot was built in a very elastic way to allow flexible bending of the parts,[17] but the disadvantage was an uncontrolled torsion effect that occurred when the snake lifted some of its parts. Some snake-like robots are designed like invertebrate robots by employing tendons transmitting powers, which are provided by hydraulic actuators.[18] But hydraulic schemes are not very suitable for locomoting snake-like robots because it is difficult for shape control, mechanism simplification, and micromation.[1] However, it is known that the structures of most snake-like robots have a relatively low stiffness and carrying capacity compared to other types of robots. Therefore, it is important for the design strategies to increase the stiffness and load strength.

To implement practical applications of snake-like robots, many researchers have presented novel techniques for efficient control analysis. Hirose and colleagues develop kinematics in two-dimensional motion for a number of snake-like robots constructed in their laboratory by introducing the Serpenoid curve which closely matches the shape of a snake.[19] Chirikjian and Burdick present a kinematics modeling technique[20] based on the geometric feature of hyper-redundant robots to efficiently solve the inverse kinematic problem. And based on this kinematics model, an algorithm to implement a variety of gaits[21,22] is proposed, including "sidewinding" locomotion, which is analogous to the locomotion of desert snakes. The feedback control law for the snake's head position using Lyapunov method[23] has been developed by Prautsch *et al.* on the basis of

* Corresponding author. E-mail: tszhao@ysu.edu.cn

https://doi.org/10.1017/S0263574708005195 Published online by Cambridge University Press

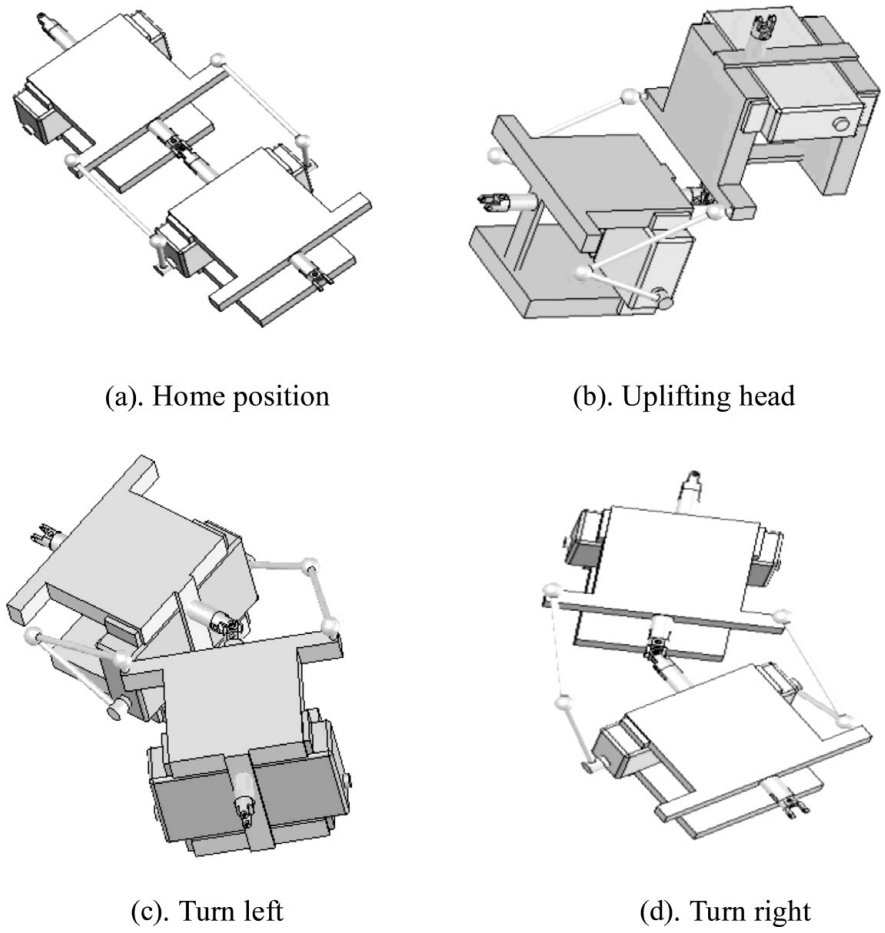


Fig. 1. 2-RSS/U spatial parallel mechanism.

the wheeled link model. Extensions to the analysis of the dynamic and actuator,[24,25] which broaden the applicability of the control theory on snake-like robots, generate a viable foundation for modeling and real-time control of snake-like robots. Ostrowski and Burdick developed a specialized form of the dynamic equations,[26] which governs undulatory systems, based on the dynamic symmetries and kinematic constraints. The kinematics and dynamics of three-dimensional snake-like robots have been formulated by Ma to analyze the sinus-lifting creeping motion.[27] In addition, for the control of hyper-redundant mechanism, underactuated systems have attracted many researchers to study in a variety of contexts,[28–30] which utilize the dynamic coupling principle to drive joints using less input. The underactuated systems have several advantages, such as less weight, less consumption of energy, and allowing a more compact design, which benefit the snake-like robots to acquire high adaptability to environments.

This paper proposes a novel model of snake-like robots based on a spatial linkage mechanism with lower mobility. The modules of the model are linked by universal joints, and each module installs two servomotors that drive one crank respectively, and the two cranks drive another module by links with two spherical joints. The reasonable structural parameters of the mechanism are obtained by performing a kinematic simulation. The kinematics is developed and the mapping between the joint angular velocities and the servomotor angular velocities is derived from the inverse position solution. On the basis of the Serpenoid curve, the motor angles developed from the relative angle are analyzed for performing lateral undulation. And the torque of the servomotors at each moment during the serpentine motion is obtained. The experiments show that the snake-like robot with the spatial parallel mechanism has the advantages of simple architecture, less weight, and energy conservation, and it can perform lateral undulation motion and uplifting of the head.

2. Architecture Model and Parameters

The novel model of snake-like robots proposed in this paper is based on a spatial linkage mechanism, which is shown in Fig. 1. The adjacent modules of this robot are connected by universal joints, and two small servomotors are mounted on each side of every module respectively. The shaft of each servomotor mounts a crank and a link connects the crank and the adjacent module with two spherical joints. And so, they constitute a 2-RSS/U spatial parallel mechanism (R: revolute joint, S: spherical joint, U: universal joint). The spatial parallel mechanism has 2 degrees of freedom (DOF), and each two adjacent modules can perform a two-dimensional rotation by a coupling actuation of the two small servomotors mounted on each module, and the motion of the robot can be controlled accordingly. The main characteristic of the snake-like robot is that a 2-RSS/U spatial parallel mechanism is taken as the basic structure of each module. Comparing with the

https://doi.org/10.1017/S0263574708005195 Published online by Cambridge University Press

Table I. Main structure parameters.

Height of module	Width of module	Length of module	Length of crank	Length of link	Vertical angle between adjacent modules	Horizontal angle between adjacent modules
80 mm	113 mm	100 mm	45 mm	52.5 mm	±70°	±40°

servomotors during the 2-DOF universal joint mechanism, the servomotors in the 2-RSS/U mechanism are easy to be controlled for spatial 2-DOF rotation, and their installation is also facile. Comparing with the motors during the adjacent orthogonal serial mechanism, all the motors in the 2-RSS/U mechanism will work to realize lateral undulation, so the utilization ratio of servomotors rises and the 2-DOF mechanism remains compact. At the same time, in contrast to the above spatial open chain, the 2-RSS/U mechanism is a spatial closed chain mechanism, where the upload on each module of the snake-like robot is supported by coupling actuation of two motors on each module through the two RSS links. The coupling actuation structure makes the inertia effect on each module decreased comparing with that actuated by only one motor on universal joint, so the 2RSS/U mechanism has structural stability. Therefore, the structural feature brings several advantages, such as a simple and compact structure, light in weight and high utilization ratio of servomotors.

When the two cranks connected with the motors on each side of a module are in a vertical position, the forward module lands on the ground, and the two modules are considered in home position, which is illustrated in Fig. 1(a). When the two motors on a module rotate in the same direction with equal torque to make the two cranks wiggle backward, the forward module can be drawn up, and the two modules can perform the uplifting head motion like a biologic snake, which is shown in Fig. 1(b). When the two motors on the posterior module rotate in the opposite direction, the two modules can perform the turning motion shown in Fig. 1(c) and (d). When the left crank rotates forward and the right one rotates backward, the forward module will turn left; if the two cranks rotate in a reverse direction, the forward module will turn right. Supposing each two modules of the snake-like robot perform left and right turning motions continuously, then the whole body will perform a serpentine motion.

The reasonable structural parameters are obtained by performing a kinematic simulation, where the maximal angles of the horizontal direction and the vertical direction between two adjacent modules are taken as the object functions; the outline sizes of the snake-like robot and the sizes of servomotors are taken as restricted conditions. Table I gives the reasonable structural parameters.

In order to obtain less friction coefficient along the longitudinal orientation than that along tangential to the snake-like robot body, two small wheels are installed under each module. The prototype developed in this paper is composed of 9 modules and actuated by 16 small servomotors except for the head module without servomotors, as shown in Fig. 2.

The main design parameters are as follows the mass of each module is $m_i = 0.4$ kg; the radius of the wheels is $r = 6.5$ mm; the maximum torque of each servomotor is $T_m = 0.2$Nm; the battery is Ni–MH charged type with 1.2 V and the battery life is 4 h; and the forward velocity of the snake-like robot is $v = 0.1$m/s.

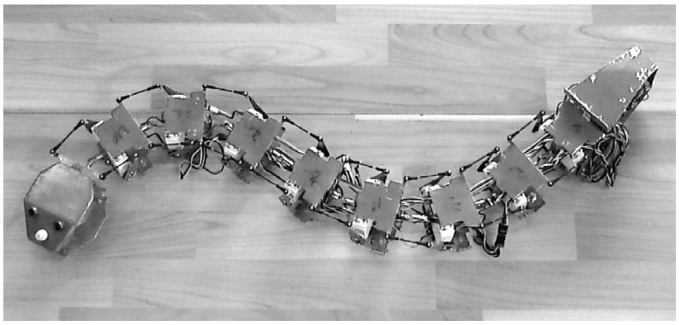


Fig. 2. Prototype of snake-like robot based on spatial linkage mechanism.

In Fig. 2, each servomotor has three wires: power, ground, and control. The voltage of the power supply is between 4 V and 6 V, and the control signals are periodic positive pulses. The high voltage lasts from 1 ms to 2 ms, the low voltage lasts from 5 ms to 20 ms. An 8515 monolithic of AVR series is applied as a microcontroller to control the angles and speed of the 16 rotations of the servomotors. The control panel and batteries are mounted on the last module of the tail. The control programs are edited and compiled on PC and then sent to the controller through RS232. The positive pulses are sent out to control 16 servomotors through interface unit PA 32–39 and PA 21–28 of the controller. The method based on monolithic of centralized control has several advantages such as easy to control, convenient to rewrite programs, and low cost.

3. Kinematics of Spatial Linkage Mechanism

In order to perform the coupling actuation of each two servomotors that are mounted on every module, the relationship between the angles of the module and the angles of the two servomotors has to be obtained first. A coordinate system shown in Fig. 3 is hence established, where origin O is at the center of the universal joint, the X-axis is in the longitudinal direction of the actuating module (on the right side), and the Z-axis is upward and vertical to the ground.

Let P_0 and Q_0 denote the centers of the spherical joints that are fixed on actuated modules, and U and V denote the intersection of the shafts of the servomotors and the central lines of the cranks, respectively. The geometric parameters from origin O to points P_0 and Q_0 are given as follows: $OE = a = 22.5$ mm, $EF = b = 27.0$ mm, $FP_0 = FQ_0 = c = 45.0$ mm, $OP_0 = OQ_0 = \sqrt{a^2 + b^2 + c^2} = 56.8$ mm. The geometric parameters from origin O to points U and V are given as $OG = d = 30.0$ mm, $GH = e = 23.0$ mm, $HU = HV = f = 45.0$ mm. The lengths of the cranks and the links are $UM_0 = VN_0 = g = 50$ mm and $P_0M_0 = Q_0N_0 = l = 52.5$ mm.

https://doi.org/10.1017/S0263574708005195 Published online by Cambridge University Press

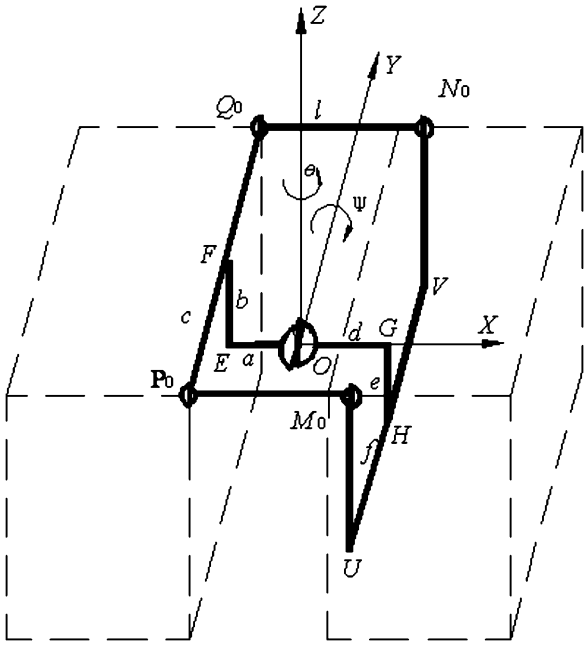


Fig. 3. Geometric parameters of joint spatial mechanism.

Suppose the left module in the above figure rotates an angle ψ about the Y-axis relative to the right module, and then rotates an angle θ about the Z-axis. After the rotation, points P_0 and Q_0 reach points P and Q, and points M_0 and N_0, the centers of spherical joints on the cranks, reach points M and N. The corresponding rotation angles of servomotors are φ_1 and φ_2. The coordinates of P and Q are given as follows:

$$\begin{cases} x_P = \sqrt{a^2+b^2+c^2}\cos\left(\arctan\dfrac{b}{\sqrt{a^2+c^2}}+\psi\right) \\ \qquad \times\cos\left[\arccos\left(\dfrac{a}{\sqrt{a^2+c^2}}+\pi+\theta\right)\right] \\ y_P = \sqrt{a^2+b^2+c^2}\cos\left(\arctan\dfrac{b}{\sqrt{a^2+c^2}}+\psi\right) \\ \qquad \times\sin\left[\arccos\left(\dfrac{a}{\sqrt{a^2+c^2}}+\pi+\theta\right)\right] \\ z_P = \sqrt{a^2+b^2+c^2}\sin\left(\arctan\dfrac{b}{\sqrt{a^2+c^2}}+\psi\right) \end{cases} \quad (1)$$

and

$$\begin{cases} x_Q = \sqrt{a^2+b^2+c^2}\cos\left(\arctan\dfrac{b}{\sqrt{a^2+c^2}}+\psi\right) \\ \qquad \times\cos\left[\arccos\left(\pi-\dfrac{a}{\sqrt{a^2+c^2}}+\theta\right)\right] \\ y_Q = \sqrt{a^2+b^2+c^2}\cos\left(\arctan\dfrac{b}{\sqrt{a^2+c^2}}+\psi\right) \\ \qquad \times\sin\left[\arccos\left(\pi-\dfrac{a}{\sqrt{a^2+c^2}}+\theta\right)\right] \\ z_Q = \sqrt{a^2+b^2+c^2}\sin\left(\arctan\dfrac{b}{\sqrt{a^2+c^2}}+\psi\right) \end{cases} \quad (2)$$

The coordinates of points M and N are given as

$$\begin{cases} x_M = d + g\cos\varphi_1 \\ y_M = -c \\ z_M = b - g\,(1-\sin\varphi_1) \end{cases} \quad (3)$$

and

$$\begin{cases} x_N = d + g\cos\varphi_2 \\ y_N = c \\ z_N = b - g\,(1-\sin\varphi_2) \end{cases}, \quad (4)$$

where φ_1 and φ_2 are the angles of the two servomotors, and they are also the angles of the two cranks rotation. On the basis of the invariance of the link length, the constraint equations can be obtained as

$$\begin{cases} (x_P-x_M)^2+(y_P-y_M)^2+(z_P-z_M)^2 = l^2 \\ (x_Q-x_N)^2+(y_Q-y_N)^2+(z_Q-z_N)^2 = l^2 \end{cases}. \quad (5)$$

Substituting (1)–(4) into (5) yields

$$\begin{cases} A_1\cos\varphi_1 + B_1\sin\varphi_1 = C_1 \\ A_2\cos\varphi_2 + B_2\sin\varphi_2 = C_2 \end{cases}, \quad (6)$$

where

$$A_i = ga - g\sqrt{a^2+b^2+c^2}\cos(\psi+\xi)\cos(\theta+\sigma_i)\,(i=1,2)$$

$$B_1 = B_2 = g(b-g-\sqrt{a^2+b^2+c^2})$$

$$C_i = -\sqrt{a^2+b^2+c^2}[c\cos(\psi+\xi)\sin(\theta+\sigma_i) - d\cos(\psi+\xi) \times\cos(\theta+\sigma_i) + e\sin(\psi+\xi)] + D \quad (i=1,2)$$

$$D = \frac{1}{2}[l^2-(a^2+b^2+c^2)-c^2-g^2-d^2-e^2]$$

$$\xi = \arctan\left(\frac{b}{\sqrt{a^2+c^2}}\right)$$

$$\sigma_1 = \arccos\frac{a}{\sqrt{a^2+c^2}} + \pi\,(\sigma_1 > \pi)$$

$$\sigma_2 = \pi - \arccos\frac{a}{\sqrt{a^2+c^2}}\,(\sigma_2 < \pi)$$

From (6), the inverse position solution of the spatial linkage mechanism can be obtained:

$$\begin{cases} \varphi_1 = \sin^{-1}\dfrac{C_1}{\sqrt{A_1^2+B_1^2}} - \sin^{-1}\dfrac{A_1}{\sqrt{A_1^2+B_1^2}} \\ \varphi_2 = \sin^{-1}\dfrac{C_2}{\sqrt{A_2^2+B_2^2}} - \sin^{-1}\dfrac{A_2}{\sqrt{A_2^2+B_2^2}} \end{cases}. \quad (7)$$

The angular velocities of the two servomotors can be obtained by differentiating (7),

$$\begin{cases} \dot{\varphi}_1 = W_{11}\dot{A}_1 + W_{12}\dot{B}_1 + W_{13}\dot{C}_1 \\ \dot{\varphi}_2 = W_{21}\dot{A}_2 + W_{22}\dot{B}_2 + W_{23}\dot{C}_2 \end{cases}, \quad (8)$$

https://doi.org/10.1017/S0263574708005195 Published online by Cambridge University Press

where

$$\begin{aligned}
\dot{A}_i &= g\sqrt{a^2+b^2+c^2}[\sin(\psi+\xi)\cos(\theta+\sigma_i)\,\dot{\psi} \\
&\quad +\cos(\psi+\xi)\sin(\theta+\sigma_i)\,\dot{\theta}] \quad (i=1,2) \\
\dot{B}_1 &= \dot{B}_2 = -g\sqrt{a^2+b^2+c^2}\cos(\psi+\xi)\,\dot{\psi} \\
\dot{C}_i &= -\sin(\psi+\xi)\,\dot{\psi}[c\sqrt{a^2+b^2+c^2}\sin(\theta+\sigma_i) \\
&\quad -d\cos(\theta+\sigma_i)] - \cos(\psi+\xi)\sqrt{a^2+b^2+c^2}[e\,\dot{\psi} \\
&\quad +c\cos(\theta+\sigma_i)\,\dot{\theta}+d\sin(\theta+\sigma_i)\,\dot{\theta}] \quad (i=1,2) \\
W_{i1} &= -\frac{A_iC_i}{\left(A_i^2+B_i^2\right)\sqrt{A_i^2+B_i^2-C_i^2}} + \frac{1}{B_i} - \frac{A_i^2}{B_i\left(A_i^2+B_i^2\right)} \\
W_{i2} &= -\frac{B_iC_i}{\left(A_i^2+B_i^2\right)\sqrt{A_i^2+B_i^2-C_i^2}} - \frac{A_i^2}{B_i\left(A_i^2+B_i^2\right)}, \\
W_{i3} &= \frac{1}{\sqrt{A_i^2+B_i^2-C_i^2}} \quad (i=1,2)
\end{aligned}$$

Substituting the differentials of A_i, B_i, C_i, $(i=1,2)$, which are the functions of $\dot{\psi}$ and $\dot{\theta}$, into (8), the angular velocities of the two servomotors can be rewritten as

$$\begin{cases}
\dot{\varphi}_1 = (W_{11}L_1+W_{12}N_1+W_{13}P_1)\,\dot{\psi}+(W_{11}M_1+W_{13}Q_1)\,\dot{\theta} \\
\dot{\varphi}_2 = (W_{21}L_2+W_{22}N_2+W_{23}P_2)\,\dot{\psi}+(W_{21}M_2+W_{23}Q_2)\,\dot{\theta}
\end{cases}, \tag{9}$$

where

$$\begin{aligned}
L_i &= g\sqrt{a^2+b^2+c^2}\sin(\psi+\xi)\cos(\theta+\sigma_i) \quad (i=1,2) \\
M_i &= g\sqrt{a^2+b^2+c^2}\cos(\psi+\xi)\sin(\theta+\sigma_i) \quad (i=1,2) \\
N_i &= g\sqrt{a^2+b^2+c^2}\cos(\psi+\xi) \quad (i=1,2) \\
P_i &= \sqrt{a^2+b^2+c^2}[c\sin(\psi+\xi)\sin(\theta+\sigma_i)-d\sin(\psi+\xi) \\
&\quad \times\cos(\theta+\sigma_i)]-e\sqrt{a^2+b^2+c^2}\cos(\psi+\xi)\,(i=1,2) \\
Q_i &= -\cos(\psi+\xi)\sqrt{a^2+b^2+c^2}[c\cos(\theta+\sigma_i) \\
&\quad +d\sin(\theta+\sigma_i)] \quad (i=1,2)
\end{aligned}$$

Therefore (9) can be rewritten as

$$\begin{pmatrix}\dot{\varphi}_1\\ \dot{\varphi}_2\end{pmatrix} = J\begin{pmatrix}\dot{\psi}\\ \dot{\theta}\end{pmatrix}, \tag{10}$$

where $J=\begin{bmatrix}J_{11} & J_{12}\\ J_{21} & J_{22}\end{bmatrix}$, $J_{11}=W_{11}L_1+W_{12}N_1+W_{13}P_1$, $J_{12}=W_{11}M_1+W_{13}Q_1$, $J_{21}=W_{21}L_2+W_{22}N_2+W_{23}P_2$, $J_{22}=W_{21}M_2+W_{23}Q_2$.

4. Locomotive Gaits

Lateral undulation is a common motion pattern performed by most snakes on the flat terrain. The characteristic of this locomotion is the propagation of sinus-like crawling action along the body of snake-like robots, and it has several advantages such as simple motion form and high efficiency. Consider the snake-like robot perform planar locomotion of lateral undulation, that is, let the joint angles for vertical movement be zero, $\psi_i = 0 (i=1,\ldots,8)$. From Professor Hirose's suggestion,[19] the Serpenoid curve can be used as the basic backbone curve of a snake-like robot when it creeps in traveling wave locomotion. The coordinates of any point on the Serpenoid curve can be obtained from the following expression:

$$\begin{cases}
x(s) = \displaystyle\int_0^s \cos(\xi_\sigma)\,d\sigma \\
y(s) = \displaystyle\int_0^s \sin(\xi_\sigma)\,d\sigma
\end{cases}, \tag{11}$$

where $\xi_\sigma = a\cos(b\sigma)+c\sigma$; a, b, and c are scalars; and a determines the initial winding angle of the curve, b determines the number of periods in a unit length and amplitude, and c determines the curvature of a unit Serpenoid curve.

The Serpenoid curve can also be represented approximatively in terms of successively connected n segments (modules) with length L/n, which are proposed by Saitio *et al.*,[31] and also the following formulas. Consider $n+1$ points on the curve specified by $s_i = iL/n (i=0,\ldots,n)$, and the values of $x(s_i)$ and $y(s_i)$ can be approximately obtained as

$$\begin{cases}
x_i = \displaystyle\sum_{k=1}^{i}\frac{L}{n}\cos\left[a\cos\left(\frac{kb}{n}\right)+\frac{kc}{n}\right] \\
y_i = \displaystyle\sum_{k=1}^{i}\frac{L}{n}\sin\left[a\cos\left(\frac{kb}{n}\right)+\frac{kc}{n}\right]
\end{cases}. \tag{12}$$

The angles of each segment measured from the X-axis in a counterclockwise manner can be obtained based on the values of coordinates that describe the position of the segments' endpoints. Therefore, the relative angle of each two segments can be given as

$$\theta_i = \alpha\sin\left(i\beta+\frac{\beta}{2}\right)+\gamma \quad (i=1,\ldots,n-1), \tag{13}$$

where $\alpha = a|\sin(\beta/2)|$, $\beta = b/n$, and $\gamma = -c/n$. When scalars a, b, and c have different values, the shape of the Serpenoid curve is different. Thus, if each relative angle (joint angle) between the two modules changes in the sinusoidal manner shown in (13), the snake-like robot will perform lateral undulation in terms of the Serpenoid curve. On the basis of the periodicity of the sine function, the relative angle can be written as

$$\theta_i(t) = \alpha\sin\left(\omega t+i\beta+\frac{\beta}{2}\right)+\gamma \quad (i=1,\ldots,n-1), \tag{14}$$

where ω specifies how fast the serpentine wave propagates along the body; β also affects the propagation speed. At each moment, the values of these relative angles still satisfy the sinusoidal regularity. Therefore, the continuous serpentine

https://doi.org/10.1017/S0263574708005195 Published online by Cambridge University Press

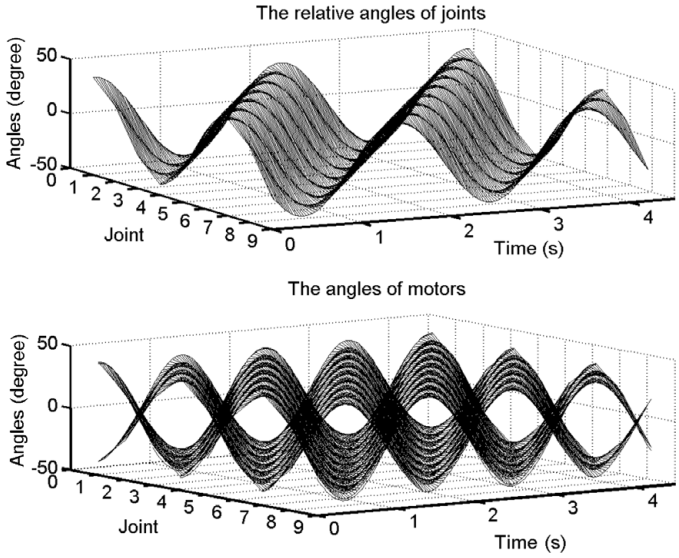


Fig. 4. Relative angles of joints and angles of motors during a lateral undulation period.

motion can be imitated by changing the relative angles of the snake-like robot according to (14).

When the snake-like robot performs lateral undulation with different serpentine shapes, the angles of each of the two servomotors on every 2-RSS/U modular can be obtained based on (7), (14), and the reasonable structural parameters. These angles of the servomotors can be employed for the controller to plan the motion patterns of the snake-like robot, which means angles control.

4.1. Lateral undulation

The prototype shown in Fig. 2 is composed of nine modules, so $n = 9$; when the scalars are specified as $a = \pi/4, b = 6\pi$, $c = 0, \omega = 3\text{rad/s}$, the relative angles at each moment during the process of lateral undulation can be expressed as $\theta_i(t) = \frac{\sqrt{3}}{8}\pi \sin(3t + \frac{2}{3}\pi i + \frac{1}{3}\pi)(i = 1, \ldots, 8)$ and the period of the relative angles is $T = 2\pi/\omega \approx 2.1$ s.

When a snake-like robot performs lateral undulation, the relative angles between each two modules and the angles of each motor on the robot can be obtained from (7) and (14), which are shown in Fig. 4. The varying regularity of the relative angles at each moment lies on a sinusoidal curve face, and the angles of left motors on each module also change on a sinusoidal curve face that coincides with that of the relative angles. On the basis of the characteristic of the 2-RSS/U mechanism, the rotary direction of each two motors on the modules is opposite during the lateral undulation motion, therefore, the angles of the right motors change on an opposite sinusoidal curve face to that of the left ones.

4.2. Lateral undulation with turning

Let the parameters be specified as $a = \pi/4, b = 6\pi, c = 1$; the corresponding relative angles can be expressed as $\theta_i(t) = \frac{\sqrt{3}}{8}\pi \sin(3t + \frac{2}{3}\pi i + \frac{1}{3}\pi) + \frac{1}{9}(i = 1, \ldots, 8)$ and the snake-like robot performs a left turning motion. The angles of each motor on the snake-like robot during left turning motion can be obtained from (7), which are shown in Fig. 5. When the snake-like robot performs the left turning motion, the varying regularity of the relative angles still lies on a standard

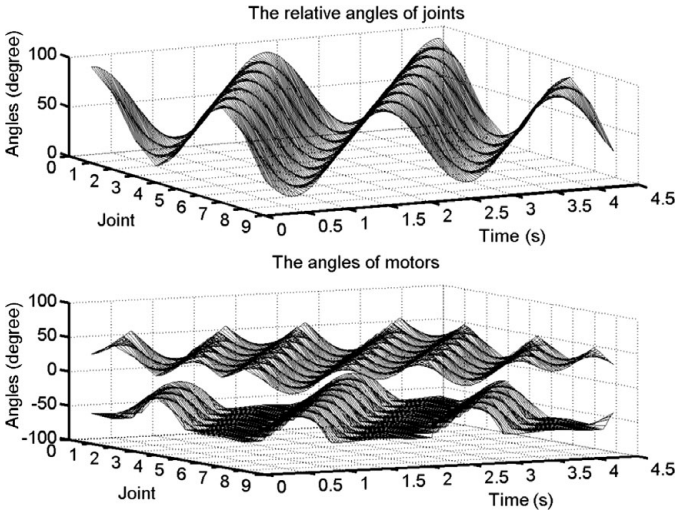


Fig. 5. The relative angles of joints and angles of each motor during left turning motion.

sinusoidal curve face with excursion compared with that of the lateral undulation, as shown in the top part of Fig. 5. But the regularities of motor angles have changed, which appear as normal waviness faces but not sinusoidal curve faces. As shown in the bottom part of Fig. 5, the upper curve face describes the angles of left motors, whose alteration of wave crest and wave hollow is faster than that of the relative angles, and the change of the angles of right motors becomes slow. The minimum of left motors angles correspond to that of relative angles, when the right motors angles are in maximum.

These curved faces indicate that the change of the left motor angles is faster than that of the right ones during the lateral undulation with left turning, and the left motors on the snake-like robot fill the role of turning.

Let the parameters be specified as $a = \pi/4, b = 6\pi, c = -1$; the corresponding relative angles can be expressed as $\theta_i(t) = \frac{\sqrt{3}}{8}\pi \sin(3t + \frac{2}{3}\pi i + \frac{1}{3}\pi) - \frac{1}{9}(i = 1, \ldots, 8)$ and the robot performs a right turning motion. The angles of each motor during right turning motion can be obtained from (7), as shown in Fig. 6. When the snake-like robot

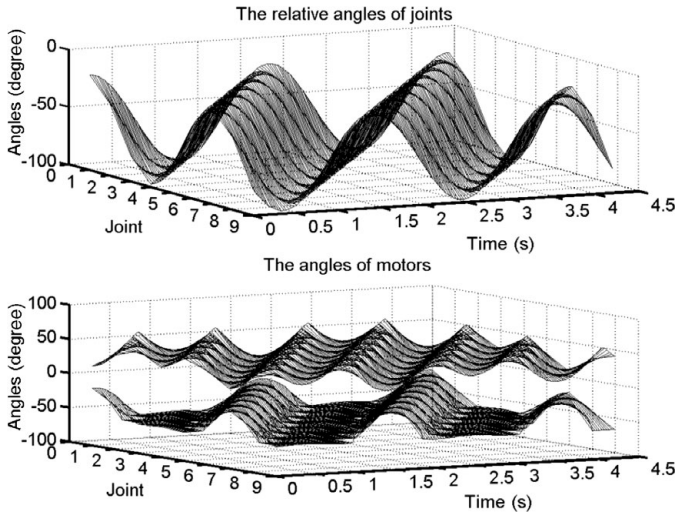


Fig. 6. The relative angles of joints and angles of each motor during right turning motion.

https://doi.org/10.1017/S0263574708005195 Published online by Cambridge University Press

performs the right turning motion, the varying regularity of the relative angles lies on a sinusoidal curve face with excursion compared with that of the lateral undulation.

The angular regularity of the left motors is similar to that of the right motors during the left turning motion, as shown as the top curve face in the bottom part of Fig. 6, and the regularity of the right motors is similar to that of the left ones, which indicates that the right motors on the snake-like robot fill the role of turning during lateral undulation with right turning.

5. Torques Analysis

From the mechanism analysis in this paper, the snake-like robot can perform planar lateral undulation based on the coupling actuation of two servomotors on each module. The torque calculations of two motors on each module will be analyzed in this section. On the basis of the analysis in Section 2, when the two cranks are in vertical position, the two modules are considered in home position. The geometric parameters of the two modules are shown in Fig. 7.

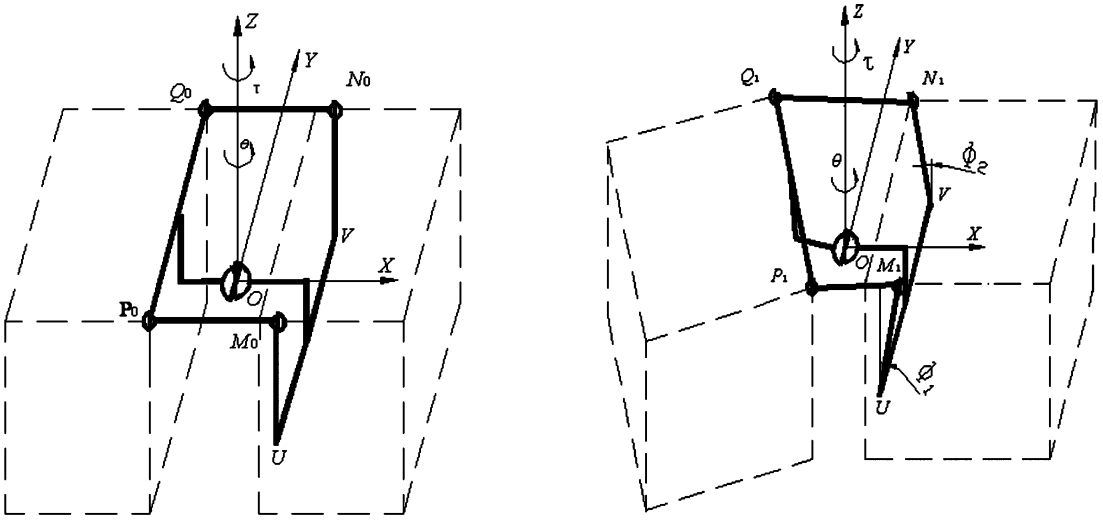
Suppose a torque τ acts on the Z-coordinate axis of the universal joint between the two modules and the right module in Fig. 7 be fixed to the ground surface; then this torque makes the left module rotate an angle θ about Z-axis, and so the torque can be expressed as $\tau(t) = \mathrm{I}_Z\ddot{\theta}(t)$, where I_Z represents the moment of inertia of each module around the Z-axis of the universal joints during each two adjacent modules, that is, the moment of inertia can be obtained by assuming the module as a cylinder rotating around a fixed axis, and based on the given structural parameters $I_Z = 1.33 \times 10^{-3}\,\mathrm{kg}\cdot\mathrm{m}^2$. According to the moment balance theory, the total torques produced by the two motors on the right module must be equal to the torque $\tau(t)$. Because the rotary directions of the two motors are opposite, the forces acting on the two cranks are couples, which can be expressed as $M(t) = F(t)l_{PQ}$ (l_{PQ} represents the width of the module) and $M(t) = \tau(t)$.

On the basis of the geometric characteristic of the 2-RSS/U mechanism and moment balance, the torque produced by the left motor can be expressed as $T_1(t) = F(t)l_{MU}\cos(\varphi_1)$ (l_{MU} represents the length of the crank). According to the analysis above and the geometric parameters obtained in Section 2, the torque produced by the left motor can be rewritten as $T_1(t) = \mathrm{I}\ddot{\theta}(t)l_{MU}/l_{PQ}\cos(\varphi_1)$, and the torque produced by the right motor can be obtained similarly. Therefore, when the $(i-1)$th module rotates an angle θ about the Z-axis, ignoring the influence of friction, the torques produced by the two motors on the ith module can be obtained as

$$T_{i,j}(t) = \mathrm{I}\ddot{\theta}_i(t)\frac{l_{MU}}{l_{PQ}}\cos(\varphi_j) \quad (i = 1, \ldots, 9;\ j = 1, 2). \tag{15}$$

From (15), when the locomotive gait of the snake-like robot is determined, the torques produced by motors are relative to the structural parameters, such as rotary inertia of a module and the ratio of the length of crank and the width of module. On the basis of the analysis of the locomotive gaits in Section 4, the corresponding torques of motors can be obtained, which are illustrated as follows.

As shown in Fig. 8, the torques produced by two motors on each module are in opposite direction with equal value at each moment during lateral undulation. Meanwhile the plots of the motor torque are similar to those of the angles in the above section when the structural and relative joint angle parameters are specified with only time-shifts, that states the torque of motors change depending on the relative joint angles during lateral undulation. According to the structural parameters, the maximum value of the horizontal angle between adjacent modules is $\theta_m = 40^\circ$, that is, $\alpha_m = 2\pi/9$; based on (14), $\ddot{\theta}_i(t) = -\alpha\omega^2\sin(\omega t + i\beta + \beta/2)(i = 1, \ldots, 8)$; when the scalars are specified as fixed values, $\beta = 2\pi/3$ and $\omega = 3\,\mathrm{rad/s}$, the maximum value of the relative angular acceleration of joints can be obtained as $|\ddot{\theta}_i(t)|_m =$



(a). Home position (b). Left turning position

Fig. 7. The position of two modules during lateral undulation.

https://doi.org/10.1017/S0263574708005195 Published online by Cambridge University Press

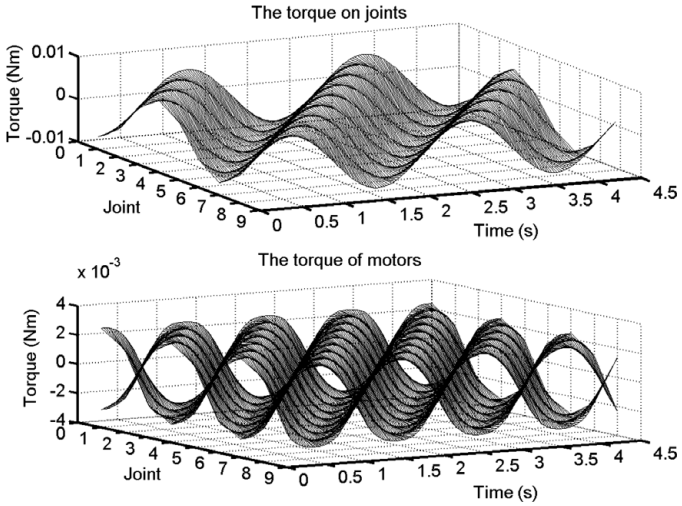


Fig. 8. The torque of motors and the equivalent torque on universal joints during lateral undulation.

$\alpha_m\omega^2(t = \frac{6n-4i+1}{18}\pi, i \le 3n/2, n \in N, i = 1, \ldots, 8)$, and so $|\ddot{\theta}_i(t)|_m = 9\alpha_m = 2\pi/3(i = 1, \ldots, 8)$. Based on (7) and (15), the maximal torques of two motors on each module can be given as $|T(t)_{i,1}|_m = |T(t)_{i,2}|_m = 3.6 \times 10^{-3}$ Nm $(t = \frac{6n-4i+1}{18}\pi, i \le 3n/2, n \in N, i = 1, \ldots, 8)$, and the equivalent torque on the Z-coordinate axis of the universal joint can be obtained as $\tau_m = 8.37 \times 10^{-3}$Nm. It is found that $|T_j|_m < \frac{1}{2}\tau_m(j = 1, 2)$, which indicates that the torque of the coupling actuation of two servomotors on each module is larger than the algebraic sum of the torques produced by these two motors; thus this 2-RSS/U spatial mechanism has an advantage of energy conservation. And the characteristic also reduces the limit of the requirement for maximum power, which would be propitious to the micromation of snake-like robots.

The comparisons of the torque of the motors and the equivalent torque on universal joints when the snake-like robot performs lateral undulation with turnings are illustrated in Fig. 9. The equivalent torque on universal joints changes on a standard sinusoidal curve face, with different excursions during left and right turning motions.

During the turning motions, the torques produced by the left motors and the right motors are always in opposite direction with equal values, and the torque of the left motors is positive during left turning motion and negative during right turning motion. This characteristic makes the torque control prone to be realized during lateral undulation.

6. Experimental Validation

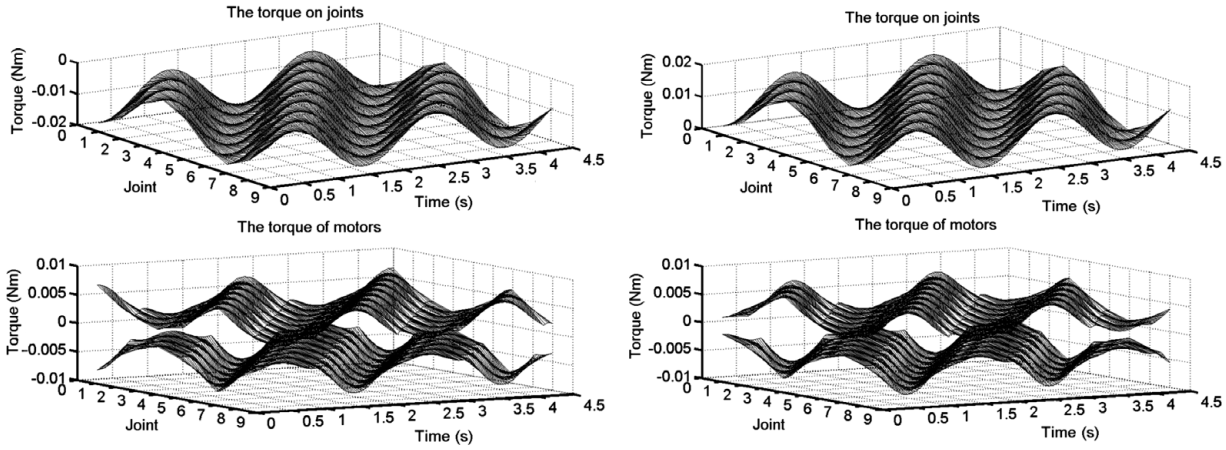
To show the validity of the developed simulation that analyzed the locomotive gaits and torque of motors of the snake-like robot on a plane, a prototype of snake-like robot is manufactured and several experiments about lateral undulation are conducted according to the motion pattern planning and torque analysis above.

6.1. Lateral undulation

The input angles of motors on each module can be obtained, according to the formulas (7) and (14), when the scalars are specified as the same as in Section 4: $\alpha = \sqrt{3}\pi/8, \beta = 2\pi/3, \gamma = 0, \omega = 3$ rad/s; hence the velocity of the prototype along the robot body can be obtained as $v = 0.1$ m/s. The experiment of lateral undulation is conducted as shown in Fig. 10, where axis L_r (r-reference) represents the direction along the texture of the floorboard; the dashed line is parallel to L_a (a-axis of motion) which denotes the axis of lateral undulation of the snake-like robot. Thus the angles between axes L_r and L_a describe quantitatively the locomotion of the snake-like robot by considering the ground as reference (it is similar in the figures which show the paths of left turning motion and right turning motion of the snake-like robot). Let the angles be positive measured from the axis L_r in a counterclockwise manner, then $\eta_1 = 33^\circ$, $\eta_2 = 33^\circ$, $\eta_3 = 33^\circ$—therefore $\eta_1 = \eta_2 = \eta_3$. It is demonstrated that the snake-like robot wriggles along the axis L_a in the form of a Serpenoid curve.

6.2. Lateral undulation with turning

The experiment of left turning motion is conducted as shown in Fig. 11, where the axis L_a is parallel to the axis L_r in the



(a). The torque in left turning motion (b). The torque in right turning motion

Fig. 9. The torque of motors and the equivalent torque on universal joints during lateral undulation with turnings.

https://doi.org/10.1017/S0263574708005195 Published online by Cambridge University Press

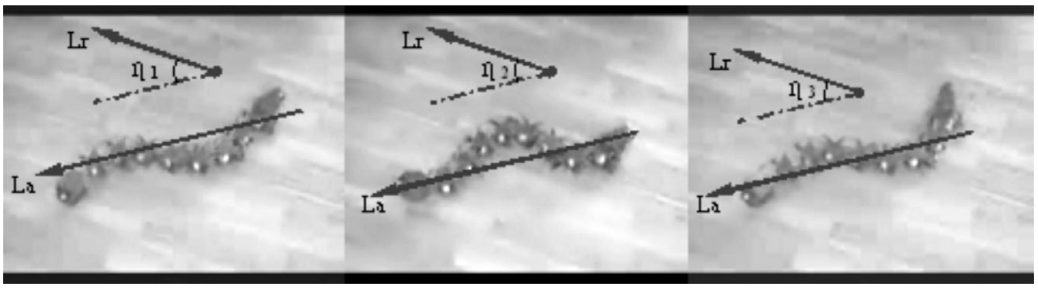


Fig. 10. The experiment on lateral undulation.

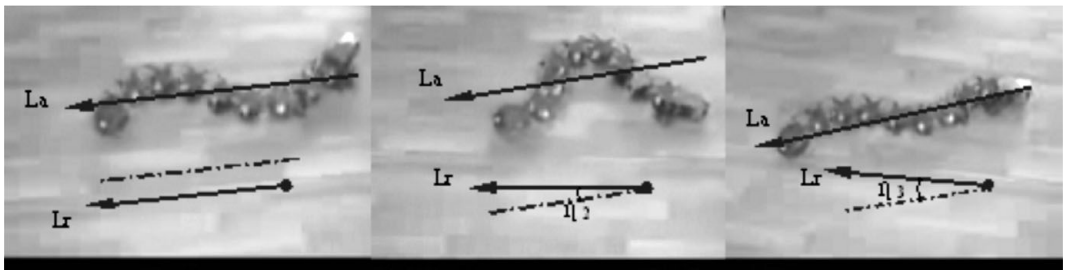


Fig. 11. The experiment on lateral undulation with left turning.

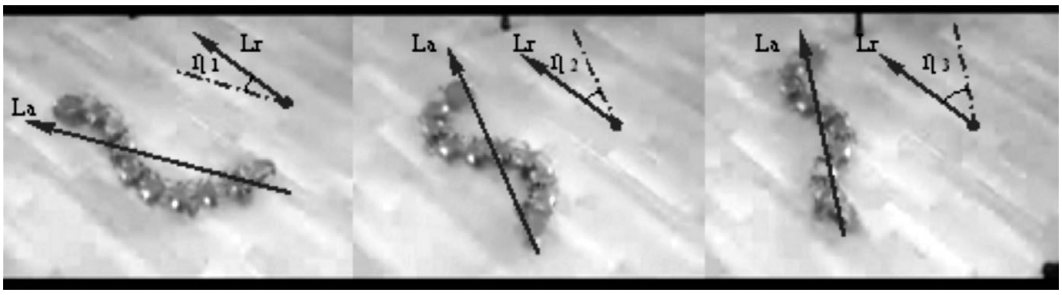


Fig. 12. The experiment on lateral undulation with right turning.

first part; therefore $\eta_1 = 0^\circ$, $\eta_2 = 10^\circ$, and $\eta_3 = 17^\circ$. The increased value of the angles between the axes of L_a and L_r demonstrates the lateral undulation with left turning of the snake-like robot.

The experiment of right turning motion is conducted as shown in Fig. 12, where $\eta_1 = 20^\circ$, $\eta_2 = -28^\circ$, and $\eta_3 = -42^\circ$. The decreased value of the angles between the axes of L_a and L_r demonstrates the lateral undulation with right turning of the snake-like robot.

The above experiments indicate that the snake-like robot as developed in this paper has the capability to realize lateral undulation, left turning motion, and right turning motion. The experimental results are thus desirable and also in conformity to the locomotive gaits. Meanwhile the snake-like robot can realize other motion modes, including uplifting of the head, and original turning motion. When the robot uplifts, it can only uplift its head and the first module because of insufficient driving moment. When it uplifts more than three modules, the middle part of the snake-like robot will hump up because of the influence of gravity, the improvement of which will be considered in the future.

7. Conclusions

This paper presents a new model of snake-like robots based on the 2-RSS/U spatial parallel mechanism. Compared with the snake-like robots based on adjacent orthogonal serial mechanism, the proposed model has the advantages of simple architecture and less weight. The model also has the characteristics of parallel mechanism, such as high stiffness, stability, and sufficient carrying capacity. By the coupling actuation of two servomotors on each module, larger torque can be obtained for each joint, and thus low power servomotors can be used for actuation and energy consumption can be reduced accordingly. With the spatial parallel mechanism, the snake-like robot can realize three-dimensional motions such as lateral undulation, left turning, right turning, and uplifting of the head. The kinematics model of the robot provides a basis for analysis of the locomotive gaits. The relative angle equation based on the Serpenoid curve can be applied in imitation of the serpentine motion, and the regularity of the angles of servomotors during lateral undulation has been summarized. The torque of servomotors at each moment has been obtained and the advantage of

https://doi.org/10.1017/S0263574708005195 Published online by Cambridge University Press

energy conservation and larger coupling torque has been proved accordingly. The corresponding experimental results show that the model based on the 2-RSS/U spatial parallel mechanism is reasonable and the kinematic solution and relative angle equation for the path planning are correct and feasible.

Acknowledgment

This research is supported by the Natural Science Fund Committee of China under grants 50375134, and 50675191.

References

1. G. S. Chirikjian, "Theory and Applications of Hyper-redundant Robotic Mechanisms," *Eight World Congress on the Theory of Machines and Mechanisms* (Society of Czechoslavak Mathematicians and Physicists, Prague, Cechoslovakia, 1991).
2. G. S. Chirikjian, "Design and Experiments with a 30 DOF Robot," *IEEE Conference on Robotics and Automation,* Vol. 3. (IEEE, NY, 1993) pp. 113–119.
3. M. Yim, "A Reconfigurable Modular Robot with Many Modes of Locomotion," *JSME International Conference on Advanced Mechatronics*, Tokyo, Japan (1993).
4. M. Yim, D. G. Duff and K. D. Roufas, "Polybot: A Modular Reconfigurable Robot," *IEEE International Conference on Robotics and Automation*, San Francisco, CA (2000).
5. S. Murata, E. Yoshida, K. Tomita, H. Kurokawa, A. Kamimura and S. Kokaji, "Hardware Design of Modular Robotic System," *IEEE/RSJ International Conference on Intelligent Robots and Systems (IROS'00)*, Takamatsu, Japan (2000).
6. S. Murata, H. Kurokawa, E. Yoshida, K. Tomita and S. Kokaji, "A 3-d Self-reconfigurable Structure," *IEEE International Conference on Robotics and Automation (ICRA'98)*, Leuven, Belgium (1998).
7. D. Rus and M. Vona, "Self-reconfiguration Planning with Compressible Unit modules," *IEEE International Conference on Robotics and Automation* (Detroit, MI, 1999).
8. P. Will, A. Castano and W. M. Shen, "Robot Modularity for Self-reconfiguration," *SPIE International Symposium on Intelligent System and Advanced Manufacturing,* Vol. 3839. (SPIE, Washington, 1999) pp. 236–245.
9. I. D. Walker, "Some Issues in Creating Invertebrate Robots," *International Symposium on Adaptive Motion of Animals and Machines*, Montreal, Canada (2000).
10. K. Togawa, M. Mori and S. Hirose, "Study on 3-dimensional Active Cord Mechanism: Development of ACM-U," *IEEE International Conference on Intelligent Robots and Systems*, Changsha, China (2000).
11. NASA. Snakebot. On-line. Available from http://amesnews.arc.nasa.gov/releases/2000/00_66AR.html
12. A. Wolf, H. Choset and B. H. Brown, "Design and control of a mobile hyper-redundant urban search and rescue robot," *Adv. Rob.* **19**(3), 221–248 (2005).
13. G. Endo, K. Togawa and S. Hirose, "Study on Self-contained and Terrain Adaptive Active Cord Mechanism," *IEEE International Conference on Intelligent Robots and Systems*, Piscataway, NJ, USA (1999) pp. 1399–1405.
14. S. G Ma, "Analysis of Snake Movement Form for Realization of Snake-like Robots," *IEEE International Conference on Robotics and Automation*, Detroit, Michigan (1999).
15. B. Klaassen and K. L. Paap, "GMD-SNAKE2: A Snake-like Robot Driven by Wheels and a Method for Motion Control," *IEEE International Conference on Robotics and Automation*, Detroit, Michigan (1999).
16. G. Miller, "A snake robot search-and-rescue mission," http://www.snakerobots.com/S5.html
17. GMD-snake, "Robot-snake with flexible real-time control," German National Research Center for Information Technology, http://ais.gmd.de/BAR/snake.html (1999).
18. G. Robinson and J. B. C. Davies, "Continuum Robots – a State of the Art," *IEEE International Conference on Robotics and Automation*, Detroit, MI (1998) pp. 2849–2854.
19. S. Hirose, "Snake-like Locomotors and Manipulators," *Biologically Inspired Robots* (Oxford University Press, New York, 1993).
20. G. S. Chirikjian and J. W. Burdick, "A modal approach to hyper-redundant manipulator kinematics," *IEEE Trans. Rob. Automat.* **10**(3), 343–354 (1994).
21. G. S. Chirikjian and J. W. Burdick, "The kinematics of hyper-redundant robotic locomotion," *IEEE Trans. Rob. Automat.* **11**(6), 781–793 (1995).
22. J. W. Burdick, J. Radford and G. S. Chirikjian, "A sidewinding locomotion gait for hyper-redundant robots" *Adv. Rob.* **9**(3), 195–216 (1995).
23. P. Prautsch, T. Mita and H. Yamaucbi, *et al.*, "Control and Analysis of the Gait of Snake Robots," *IEEE International Conference on Control Applications*, Hawaii (1999).
24. I. A. Gravagne and I. D. Walker, "Large deflection dynamics and control for planar continuum robots," *IEEE/ASME Trans. Mechatron.* **8**(2), 299–307 (2003).
25. B. A. Jones and I. D. Walker, "Practical kinematics for real-time implementation of continuum robots," *IEEE Trans. Rob.* **22**(6), 1087–1099 (2006).
26. J. Ostrowski, J. Burdick and A. D. Lewis, "Mechanics of Undulatory Locomotion: The Mixed Kinematic and Dynamic Case," *IEEE International Conference on Robotics and Automation*, Nagoya, Japan (1995).
27. S. G. Ma, O. Yoshihiro and I. Kousuke, "Dynamic Analysis of 3-dimensional Snake Robots," *IEEWSl International Conference on Intelligent Robots and Systems*, Sendai, Japan (2004).
28. M. W. Spong, "Underactuated mechanical systems" *Control Prob. Rob. Automat.* **230**, 135–150 (1998).
29. J. S. Dai and T. S. Zhao, "Stiffness characteristics and kinematics analysis of two-link elastic underactuated manipulators" *J. Rob. Syst.* **19**(4), 169–176 (2002).
30. T. S. Zhao and J. S. Dai, "Dynamics and coupling actuation of elastic underactuated manipulators" *J. Rob. Syst.* **20**(3), 135–146 (2003).
31. M. Saito, M. Fukaya and T. Iwasaki, "Serpentine locomotion with robotic snakes," *IEEE Contr. Syst. Mag.* **22**(1), 64–81 (2002).

https://doi.org/10.1017/S0263574708005195 Published online by Cambridge University Press